

ACCEPTED MANUSCRIPT

Tunable intrinsic magnetic phase transition in pristine single-layer graphene nanoribbons

To cite this article before publication: Santhosh Sivasubramani *et al* 2018 *Nanotechnology* in press <https://doi.org/10.1088/1361-6528/aadcd8>

Manuscript version: Accepted Manuscript

Accepted Manuscript is “the version of the article accepted for publication including all changes made as a result of the peer review process, and which may also include the addition to the article by IOP Publishing of a header, an article ID, a cover sheet and/or an ‘Accepted Manuscript’ watermark, but excluding any other editing, typesetting or other changes made by IOP Publishing and/or its licensors”

This Accepted Manuscript is © 2018 IOP Publishing Ltd.

During the embargo period (the 12 month period from the publication of the Version of Record of this article), the Accepted Manuscript is fully protected by copyright and cannot be reused or reposted elsewhere.

As the Version of Record of this article is going to be / has been published on a subscription basis, this Accepted Manuscript is available for reuse under a CC BY-NC-ND 3.0 licence after the 12 month embargo period.

After the embargo period, everyone is permitted to use copy and redistribute this article for non-commercial purposes only, provided that they adhere to all the terms of the licence <https://creativecommons.org/licenses/by-nc-nd/3.0>

Although reasonable endeavours have been taken to obtain all necessary permissions from third parties to include their copyrighted content within this article, their full citation and copyright line may not be present in this Accepted Manuscript version. Before using any content from this article, please refer to the Version of Record on IOPscience once published for full citation and copyright details, as permissions will likely be required. All third party content is fully copyright protected, unless specifically stated otherwise in the figure caption in the Version of Record.

View the [article online](#) for updates and enhancements.

Tunable Intrinsic Magnetic Phase Transition in Pristine Single-Layer Graphene Nanoribbons

Santhosh Sivasubramani¹, Sanghamitra Debroy¹, Swati Ghosh Acharyya², Amit Acharyya^{1}*

1 Advanced Embedded Systems and IC Design Laboratory, Department of Electrical
Engineering, Indian Institute of Technology - Hyderabad, India

2 School of Engineering Sciences and Technology, University of Hyderabad, India

ABSTRACT:

In this letter, we report an interesting phenomenon of magnetic phase transitions (MPT) observed under the combined influence of Electric field (E) and Temperature (T) leading to thermo-electromagnetic effect on the pristine single layer zigzag graphene nanoribbon (szGNR). Density functional theory based first principle calculations have been deployed for this study on intrinsic magnetic properties of graphene. Interestingly, by tuning Electric field (E) and Temperature (T), three distinct magnetic phase para, ferro, and antiferromagnetic behaviors have been exhibited in pristine single layer zigzag Graphene NanoRibbon (szGNR). We have investigated the unrivaled positional parameters of these magnetic phase transitions. MPT occurring in the system also follows a positional trend and the change in these positional parameters concerning the size of the szGNR along with the varied E and T is studied. We propose a Bow-Tie schematic to induce the intrinsic magnetism in graphene and present the envisaged model of the processor application with the reported intrinsic MPT in szGNR. These fundamental insights on intrinsic magnetic phase transitions in graphene is an essential step towards developing graphene-based spin-transfer torque magnetoresistive random-access memory (STT-MRAMs), quantum computing devices, magnonics, and spintronic memory application.

KEYWORDS: Intrinsic Magnetism, Magnetic Phase Transition, single layer zigzag Graphene NanoRibbon (szGNR), Thermo-ElectroMagnetic Effect, Spintronic Memory Devices

1. INTRODUCTION: - Magnetic properties of low dimensional materials have gained importance by virtue of its reduced hopping tendency of electrons, increased coulomb attraction and its lightweight nature. Magnetism in graphene[1] have gained attention after the revelation of nanoscale edge effect[2], p electrons energy spectrum[3] and self-healing phenomenon[4] which is capable of driving self-sustained low power devices in spintronic and magnonics applications[5,6]. The role and the necessity of the intrinsic magnetic nature of pristine graphene in these primary applications have been the motivation for the study investigated here. As the edge terminations[7] plays a significant role in determining the magnetic properties, graphene nanoribbon[8] is the recent focus of study by the research community. Due to the chirality of low energy charge carriers in graphene, the edge localized zero energy states in zigzag graphene nanoribbons are highly degenerate[9], and this property has made zigzag graphene nanoribbons as one of the major thrust areas of research and our material choice of study[10].

The existence of the magnetic properties within graphene is still debatable[11] although the existence of magnetic phases such as Ferromagnetism[12–14] (FM), Antiferromagnetism[15,16] (AFM) and Paramagnetism[17,18] (PM) has already been proclaimed in the literature[11–17]. In general, magnetism in graphene is induced by the application of electric field, doping and structural changes. Primarily, Electric field[19–23] induces magnetic phase transition in shaped - single layer graphene[15,21,24] whereas doping leads to the introduction of charged impurities and spin-polarized effects which in turn increases the spin lifetime[25] resulting in induced magnetism[26]. Graphene growth on various substrates[27] accelerates single spin dirac fermions[28], spin textures and the dirac cones effects[29] leading to the structural change induced

1
2
3 magnetic phases. First principle calculations[30–32], Hubbard model[33–35], many-body
4 perturbation theory[15,21], LLG equations[36], DFT calculations[37,38] and Quantum Monte
5 Carlo (QMC)[39] simulations have been deployed to investigate magnetic properties of graphene.
6 Tunable magnetic properties are majorly achieved by spin polarization of the edge states[40] and
7 local atomic arrangements[41]. Studies reveal that the magnetism in zigzag edged Graphene is also
8 dependent on temperature[42–45]. Zigzag effect[36,45] leading to magnetic phase transition[24]
9 and GNR's edge spin role, width tuning effects on magnetism[14,45–47] have been widely
10 reported. Graphene nanoribbons exhibit magnetic phases when it is charged, and it stores the
11 electrons in the soliton topological phase at interface[48]. The role of zak phase and magnon effects
12 in graphene's magnetic properties has also been studied[46,49,50].
13
14
15
16
17
18
19
20
21
22
23
24
25
26

27 State of the art study on magnetism in graphene is, the application of electric field[19–22] (E)
28 and the temperature[42–45,51] (T) independently changes the properties of the material. The self-
29 dependency of E and T have not been fully explored for tuning the material properties of single
30 layer zigzag Graphene NanoRibbon (szGNR). We envisage that the combined effect of E and T
31 breaks the symmetry of the system and eventually leads to magnetic phase transitions. Hence in
32 this letter, the combination of E and T and its effects on intrinsic magnetic properties (thermo-
33 electromagnetic effect) of szGNR is investigated, which would open up new avenues for soft
34 magnetic material applications[49]. In this letter, a scheme is also proposed for the fine-tuning of
35 magnetic properties in graphene and it can be extended for other carbon allotropes. Magnetic phase
36 transitions occurring in the system with their respective positions have also been addressed,
37 expediting towards area specific computing and memory applications.
38
39
40
41
42
43
44
45
46
47
48
49
50
51

52 The 2017 Magnetism Roadmap [52] states the role of Graphene-based magnetism as the key for
53 the development of spin logic, novel devices and for transporting spin information in spintronic
54
55
56
57
58
59
60

1
2
3 circuits or for reprogrammable magneto logic devices. This metal free magnetism paves way to
4 magnonics applications. Researchers have shifted their design paradigm towards developing an
5 alternative to CMOS based computing and are looking towards graphene-based computing devices
6 where computation is expected to be performed using the induced intrinsic magnetism. In line with
7 this, our study reported here throws light on the unrivaled intrinsic magnetism of free-standing
8 szGNR. We have also presented the envisaged processor application with the findings reported
9 which we believe is of significance in the ongoing research trend.

10
11
12
13
14
15
16
17
18
19 **2. METHODS:** - Density functional theory based first principle calculations have been used to
20 investigate the magnetic properties of single layer zigzag graphene nanoribbons (szGNRs).
21 Calculations have been performed in the framework of spin density functional theory[53] as
22 implemented in quantum espresso package[54,55] as described by the exchange-correlation
23 functional GGA-PBE (Generalized Gradient Approximation)[56], (Perdew–Burke–
24 Ernzerhof)[57]. Plane wave cutoff is 45 Rydberg (Ry) and fully relativistic pseudopotentials with
25 included spin-orbital coupling have been used throughout the study. Brillouin zone has been
26 integrated with Gaussian smearing of 0.04 Ry. Convergence energy is 0.005 Ry for a 10x10x10
27 Monkhorst–Pack K point grid sampled using gamma point. The saw-tooth potential is applied
28 perpendicular to the graphene sheet, for inducing the electric field in the system. Car-Parrinello
29 molecular dynamics simulations[58] have been performed as implemented in QE code to
30 determine the temperature of the system using nose thermostat with the frequency of 65 THz and
31 with varying temperatures in kelvin. To avoid subjective interaction error and to check electron
32 correlation, magnetic phase distinction concerning the energy difference is analyzed using Broken
33 Symmetry – Density Functional Theory (DFT-BS). Exchange coupling constants have been
34 calculated by solving Kohn Sham equations in the framework of Korringa-Kohn-Rostoker (KKR)

Green's function approach. Single layer zigzag graphene nanoribbon of sizes 1x1 nm, 2.5x2.5 nm, 5x5 nm, 7.5x7.5 nm and 10x10 nm (refer Table S1.) have been used for this vacuum study with temperature varying from 50 K to 730 K (optimal range to obtain MPT at E above 0 V/Å) and the electric field from 0.08 to 5.5 V/Å (optimal range to obtain MPT at T above 0 K).

3. RESULTS AND DISCUSSION: - The following section is organized as follows: 3.1) Influence of ET on MPT 3.2) Study to confirm the magnetic phase existence and its transition 3.3) Measurement of magnetic properties and its existence 3.4) Positional parameters study of the appeared magnetic phases 3.5) Envisaged Application of the finding reported.

3.1) Influence of ET on MPT: Spin orientation, relative transition energy and density of states have been studied to identify the magnetic phases and its existence. At specific E and T, the system exhibits a unique magnetic phase (PM, FM, and AFM). Further tuning it leads to the transition from one phase to other. In the szGNR, the applied T increases with decrease in E to obtain distinct magnetic phases and T is decreased when E is increased. This material specific finding has significant potential to be used in today's 3D electronics[59] where heat dissipation is of primary concern.

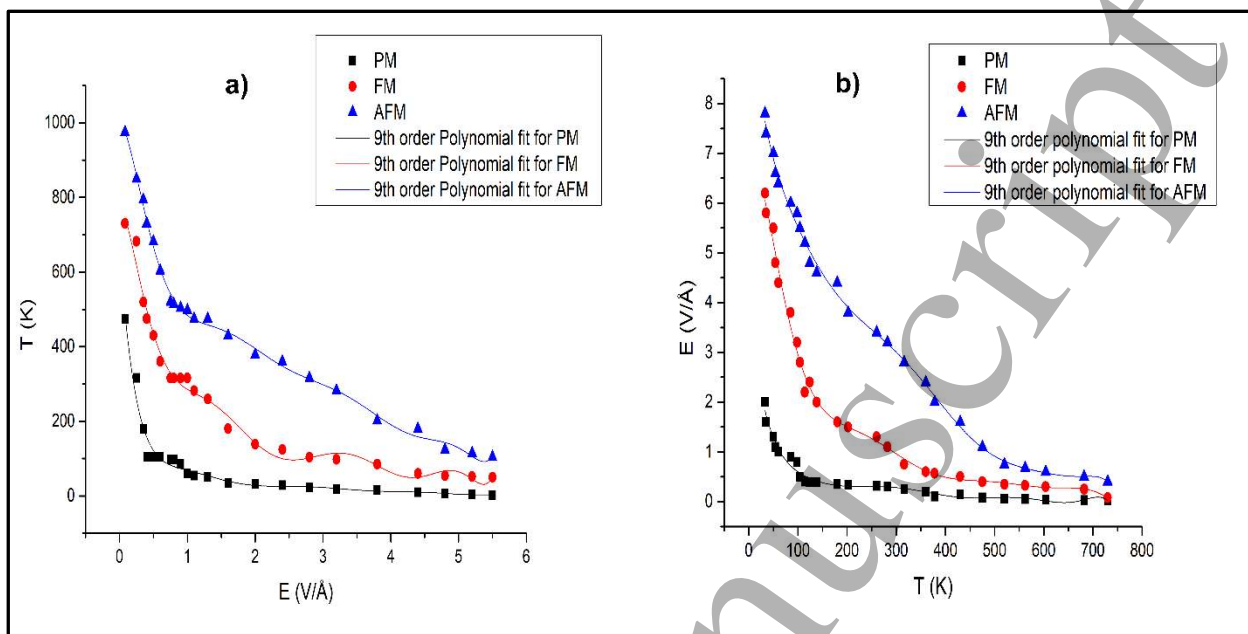


Figure 1. Electric field and temperature plot in $\text{V}/\text{\AA}$ and kelvin respectively for the magnetic phases. a) E is fixed as constant and T is varied to obtain PM, FM and AFM phases; E at $2 \text{ V}/\text{\AA}$ exhibits PM phase when $T=33 \text{ K}$, FM Phase when $T=138 \text{ K}$ and AFM phase when $T = 378 \text{ K}$ and b) T is fixed as constant and E is varied to obtain magnetic phases; T at 282 K exhibits PM phase when E is at $0.3 \text{ V}/\text{\AA}$, FM phase when E is at $1.1 \text{ V}/\text{\AA}$ and AFM phase when E is at $3.2 \text{ V}/\text{\AA}$. In the figure square represents PM phase, circle represents FM phase, and triangle represents the AFM phase. Solid lines represent the 9th order polynomial fit for the respective magnetic phases.

The combination of electric field and temperature is applied transversely to the szGNRs of length 1nm, 2.5nm, 5nm, 7.5nm and 10nm respectively. Interestingly, we note that the magnetic phase transitions occurred is independent of the size of the graphene nanoribbon (GNR). However the size of the GNR plays a role in determining the positions of the occurred magnetic phase. The corresponding E and T values for which the PM, FM and AFM phases appear is illustrated in Figure 1. As both E and T are variables, to attain a self-sustained tunable system, E is kept as constant, T is varied as shown in Figure 1(a), and T is kept as constant, E is varied as shown in Figure 1(b).

As a case study: a) The optimal values considering Advanced Micro Devices (AMD) K6-2/K6-3 processors' are as follows: With the value of E is set constant at 2.4 V/Å, szGNR needs T=29, 124, 360 K to exhibit PM, FM and AFM phases respectively. While with the emitted heat T= 316 K, szGNR requires E=0.25, 0.75, 2.8 V/Å respectively to exhibit PM, FM and AFM phase. b) The optimal values considering Intel MMX Pentium processors are as follows: With the value of E is set constant at 2.8 V/Å, szGNR needs T=22, 104, 316 K to exhibit PM, FM and AFM phases respectively. Whereas when the emitted heat (T) is 360 K, szGNR requires E=0.2, 0.6, 2.4 V/Å respectively to exhibit PM, FM and AFM phase. The electric field has been kept as constant throughout in the range of 0.08 to 5.5 V/Å and at every instance of E, the temperature has been varied to obtain the PM, FM and AFM phases respectively. Similarly, when the temperature has been kept as constant from 50K to 730K, the electric field has been varied from 0.08 to 5.5 V/Å at every instance of T, in order to obtain the PM, FM and AFM phases. These calculations have been done to ensure that both E and T are tunable to obtain the desired magnetic phase. The mathematical expression for calculating E and T values to obtain distinct magnetic phase transitions for szGNRs typically in the range of 1nm to 50 nm size is given below-

$$Y = \text{Intercept} + B1 * x^1 + B2 * x^2 + B3 * x^3 + B4 * x^4 + B5 * x^5 + B6 * x^6 + B7 * x^7 + B8 * x^8 + B9 * x^9 \quad (1)$$

Where, the values of the Intercept and B1, B2 ... B9 are given in Table 1.

Table 1. The values for E and T calculation applied in equation (1) a) with x (electric field in V/Å) as constant, respective Y (temperature in kelvin) is calculated to obtain PM, FM and AFM phases. b) with x (Temperature in kelvin) as constant respective Y (electric field in V/Å) is calculated in order to obtain PM, FM and AFM phases. No weighting factor is included in the expression, the intercepts values, and B1 to B9 values concerning the magnetic phase and their standard errors are given to reduce the error tolerability value below $\pm 2\%$.

		a) T			b) E	
Weight	No Weighting					
Residual sum of squares	7744.823 72	9696.2 6065	3332.769 38	0.1674	0.51882	0.37743
Adjusted R-square	0.94899	0.9801 1	0.99536	0.96055	0.99082	0.99569
		Value		Standard Error	Value	Standard Error
PM	Intercept	664.94718		51.68266	3.99495	0.83064
	B1	-2557.87273		529.83478	-0.09982	0.04562
	B2	4776.86221		1838.70501	0.00134	9.33723E ⁻⁴
	B3	-4938.14319		2958.84429	-1.10232E ⁻⁵	9.65708E ⁻⁶
	B4	3050.37177		2566.33073	5.75399E ⁻⁸	5.69089E ⁻⁸
	B5	-1171.34657		1295.05176	-1.91378E ⁻¹⁰	2.02E ⁻¹⁰
	B6	281.87425		391.24403	4.00235E ⁻¹³	4.38804E ⁻¹³
	B7	-41.3277		69.6504	-5.06814E ⁻¹⁶	5.69837E ⁻¹⁶
	B8	3.37432		6.73139	3.53952E ⁻¹⁹	4.05616E ⁻¹⁹
	B9	-0.11761		0.2722	-1.04437E ⁻²²	1.21597E ⁻²²
FM	Intercept	785.63736		57.8284	6.77378	1.46235
	B1	-281.9831		592.83909	0.01708	0.08031
	B2	-2777.57495		2057.35118	-0.00172	0.00164
	B3	6130.06353		3310.68974	1.97586E ⁻⁵	1.70013E ⁻⁵
	B4	-5822.33683		2871.50116	-1.09164E ⁻⁷	1.00188E ⁻⁷
	B5	3018.2759		1449.05043	3.45479E ⁻¹⁰	3.55622E ⁻¹⁰
	B6	-912.17839		437.76809	-6.58012E ⁻¹³	7.72515E ⁻¹³
	B7	160.37654		77.93274	7.46302E ⁻¹⁶	1.0032E ⁻¹⁵
B8	-15.20772		7.53184	-4.64701E ⁻¹⁹	7.14087E ⁻¹⁹	

	B9	0.6014	0.30457	1.22342E ⁻²²	2.14072E ⁻²²
AFM	Intercept	1001.77821	33.90328	10.14614	1.24727
	B1	-123.32259	347.56603	-0.11001	0.0685
	B2	-2958.85868	1206.17111	0.00136	0.0014
	B3	5663.9513	1940.97067	-1.21735E ⁻⁵	1.45008E ⁻⁵
	B4	-4884.88254	1683.48592	6.79907E ⁻⁸	8.54527E ⁻⁸
	B5	2357.14613	849.54031	-2.33751E ⁻¹⁰	3.03317E ⁻¹⁰
	B6	-675.85445	256.65196	4.91329E ⁻¹³	6.58894E ⁻¹³
	B7	114.36514	45.68993	-6.13947E ⁻¹⁶	8.55649E ⁻¹⁶
	B8	-10.54861	4.41572	4.18647E ⁻¹⁹	6.0906E ⁻¹⁹
	B9	0.40893	0.17856	-1.19972E ⁻²²	1.82587E ⁻²²

By reducing E with the increase in T and vice versa will enable the reconfigurability of the pristine szGNR based devices and making it ultra-low power. Equation (1) gives a brief mathematical explanation for the 9th order polynomial fit in Figure 1(a, b). With the value of E been known, corresponding value of T to obtain PM, FM and AFM phase in szGNR is calculated using Table 1(a) and the value of T been known the value of E is calculated using Table 1(b). Error values are specified such that the precision increases and to maintain the maximum fault tolerance in a feeble range which doesn't alter the phase transitions happening in the pristine single layer zigzag graphene nanoribbons.

3.2) Study to confirm the magnetic phase existence and its transition:

Energy barrier between the magnetic phases is overcome by the assistance of temperature. With the available literatures[42–45,51] on the effects of temperature on the magnetic properties of GNRs we realize that the energy barrier can be broken using temperature. Temperature has its

1
2
3 effects on the local coordination of atoms enabling the FM and AFM phases' in correspondence
4 to the Curie and Neel temperature. As pointed out, structural changes are possible due to the
5 varying temperature[44] which also affects the intrinsic magnetism, similarly these geometric
6 effects also assists in breaking the symmetry of the system thus leading to magnetic phases[41].
7
8 The unequal number of zig zag edges along with the temperature contributes towards the reduced
9 magnetic moment leading to phase transition. Electron depletion occurring between the two edges
10 contributes to the electron flow thus changing the magnetic moment and the difference in energy
11 density arises with the direction and the strength of the external transversely applied electric field.
12 Spins are of parallel alignment with the increase in field values in line with the Curie temperature
13 obtaining ferromagnetic phase. Similarly, the sub lattice moments are exactly opposite, but of
14 equal magnitude. The net moment obtained is zero leading to Antiferromagnetism arising above
15 the Neel temperature. With the applied field, the randomly oriented spins are aligned towards the
16 field direction and the para magnetism greatly depends on the temperature and the applied field to
17 satisfy the Curie Law. Transverse electric field is applied throughout this study reported aiding in
18 MPT backed up by the available literature [19–22] . One of the reason vertical electrical field not
19 being resolved for magnetic study is the rising magnetism is easily quenched by the thermal
20 activation. Net magnetic-moment, individual coupling constants entitling towards the different
21 magnetic phases are tabulated in Table 2. The magnetic states are determined using the relative
22 transition energy and the magnetic moment values obtained as tabulated and highlighted in the
23 revised manuscript Table 2. Magnetization values have been presented in Table S3, available in
24 the supplementary information, which aids in the determination of the magnetic phases. Magnetic
25 phase diagram represented using the contour plot observed in the Xcrysden aids in identification
26 of the spin orientations which assists to determine the magnetic phases. Magnetic moment and the
27
28
29
30
31
32
33
34
35
36
37
38
39
40
41
42
43
44
45
46
47
48
49
50
51
52
53
54
55
56
57
58
59
60

energy gap values as illustrated in Figure 2 as a function of electric field and temperature also aids in confirming the existence of magnetic phases appeared.

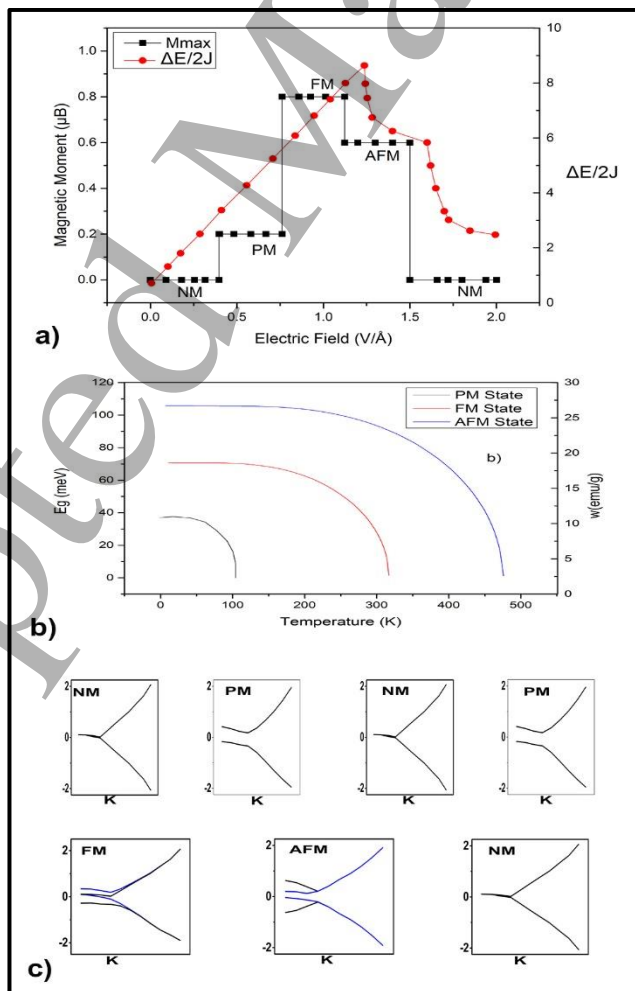
Table 2. a) Relative transition energies in (meV) in pristine szGNRs for [1x1, 2.5x2.5, 5x5, 7.5x7.5 and 10x10] nm
b) Total spin magnetic moments in (μ B) for all the magnetic phases

Pristine szGNRs dimension [n x n] in nm		[1x1]	[2.5x2.5]	[5x5]	[7.5x7.5]	[10x10]	
a)	RTE _{NM → PM}	-10	-31	-78	-114	-167	
	RTE _{PM → NM}	-28	-52	-99	-130	-189	
	RTE _{PM → FM}	-40	-102	-153	-193	-260	
	RTE _{FM → AFM}	-39	-145	-236	-382	-410	
	RTE _{AFM → NM}	-48	-115	-288	-408	-560	
b)	PM	M _{total}	0.5	0.8	1	1.2	1.4
		M _{up}	1	1.395	1.583	1.901	2.834
		M _{edge}	0.2	0.32	0.38	0.44	0.58
	FM	M _{total}	1.5	2	3	4	4.5
		M _{up}	1.658	1.92	2.497	3.567	5.089
		M _{edge}	0.198	0.249	0.275	0.291	0.358
	AFM	M _{total}	1.3	2.5	4	4.3	4.8
		M _{up}	1.477	1.6	1.743	2.782	4.005
		M _{edge}	0.15	0.22	0.27	0.29	0.34

DFT-BS calculations and Kohn Sham equations using KKR Green's function approach[60] is used to analyze the relative transition energies (RTE) and to verify the existence of the magnetic phases along with its translational positional parameters. As edge terminations plays a major role in the internal magnetism of szGNR, its spin states are also studied to understand its behavioral changes. Five varied dimensions of szGNR have been studied and observed that the magnetic

phase transition occurring was uniform for all the cases and the magnetic strength changes logarithmically from small dimension to large dimension. Relative translational energy as listed in Table 2(a) for PM \rightarrow FM transition is stronger compared to the other transitions. The NM \rightarrow PM transition is the strongest of all. FM \rightarrow AFM transition is equally comparable with the PM \rightarrow FM transition. Still, the total magnetic moment obtained is in par with the soft magnetic materials[61]. Stability of the magnetic phases are as follows: FM>PM>AFM. The ground state NM is achieved after every complete transition cycle, enabling the reversible nature of the system. FM state is more stable compared to PM and AFM which is quite evident from the magnetic moment values listed in Table 2(b).

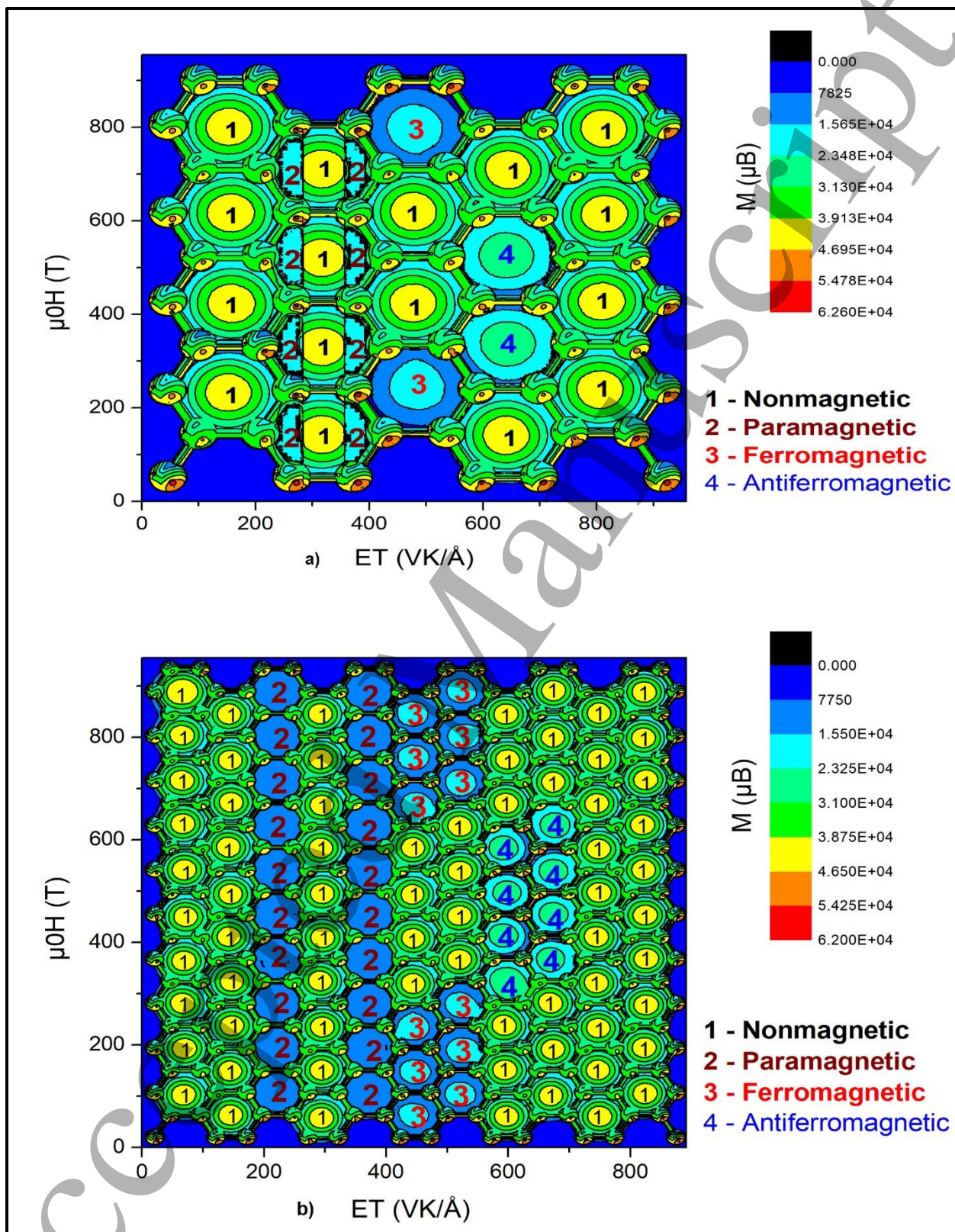
3.3) Measurement of magnetic properties and its existence:



1
2
3 **Figure 2.** a) Highest local Magnetic moment and ratio of energy split to the magnetic states as a function of the
4 applied external electric field (Transverse) and the tunable magnetic phase transitions (MPT) with respective field
5 applied and their corresponding magnetic moments. b) Relationship between electronic band gap (E_g), normalized
6 vector (w) and Temperature for three inter-dependent magnetic phase transitions as a function of localized spin
7 moments. c) Band diagram of different magnetic phases (NM-PM-FM-AFM-NM) black solid line representing spin
8 down and the blue solid line representing spin up
9
10
11
12
13
14

15 In the absence of an electric field and temperature, the ground state is NM as tabulated in Table.
16
17 2. Local maxima contributing towards the largest local magnetic moment (M_{max}) along with the
18 difference in energy ($2J$) and the single particle energy splitting (ΔE) with varying electric field is
19 presented in Figure 2(a). The dramatic transition from PM- \rightarrow FM and AFM- \rightarrow NM for the applied
20 field with the temperature value set as constant is acquainted by the kinetic energy induced. The
21 normalized vector component resolving the orientation of spin directions with the energy gap is
22 illustrated in Figure 2(b) as a function of temperature. Figure 2(c) illustrates the band diagram of
23 the exhibited magnetic phases with the NM state showing zero band gap.
24
25
26
27
28
29
30
31
32

33 Magnetic phase diagram capturing the phase transitions is illustrated as shown in Figure 3. The
34 magnetization values have been used to present the contour plot against the magnetic intensity and
35 the product of electric field and temperature (represented as ET in this paper). Numbers 1, 2, 3, 4
36 have been superimposed on the contour plot distinguishing the phases NM, PM, FM, and AFM
37 respectively. Pristine single layer zigzag graphene nanoribbons of length 1×1 , 2.5×2.5 and 5.5 nm
38 have been studied here. In addition to this 7.5×7.5 and 10×10 nm szGNR have been discussed in
39 the supplementary info available (tabulated in Table S2). Magnetic Phase transition occurring
40 follows a positional trend. The appeared MPT is repeated and increased logarithmically for all the
41 five dimensions reported. For magnetization values of all states refer Table S3 available as
42 supplementary info.
43
44
45
46
47
48
49
50
51
52
53
54
55
56
57
58
59
60



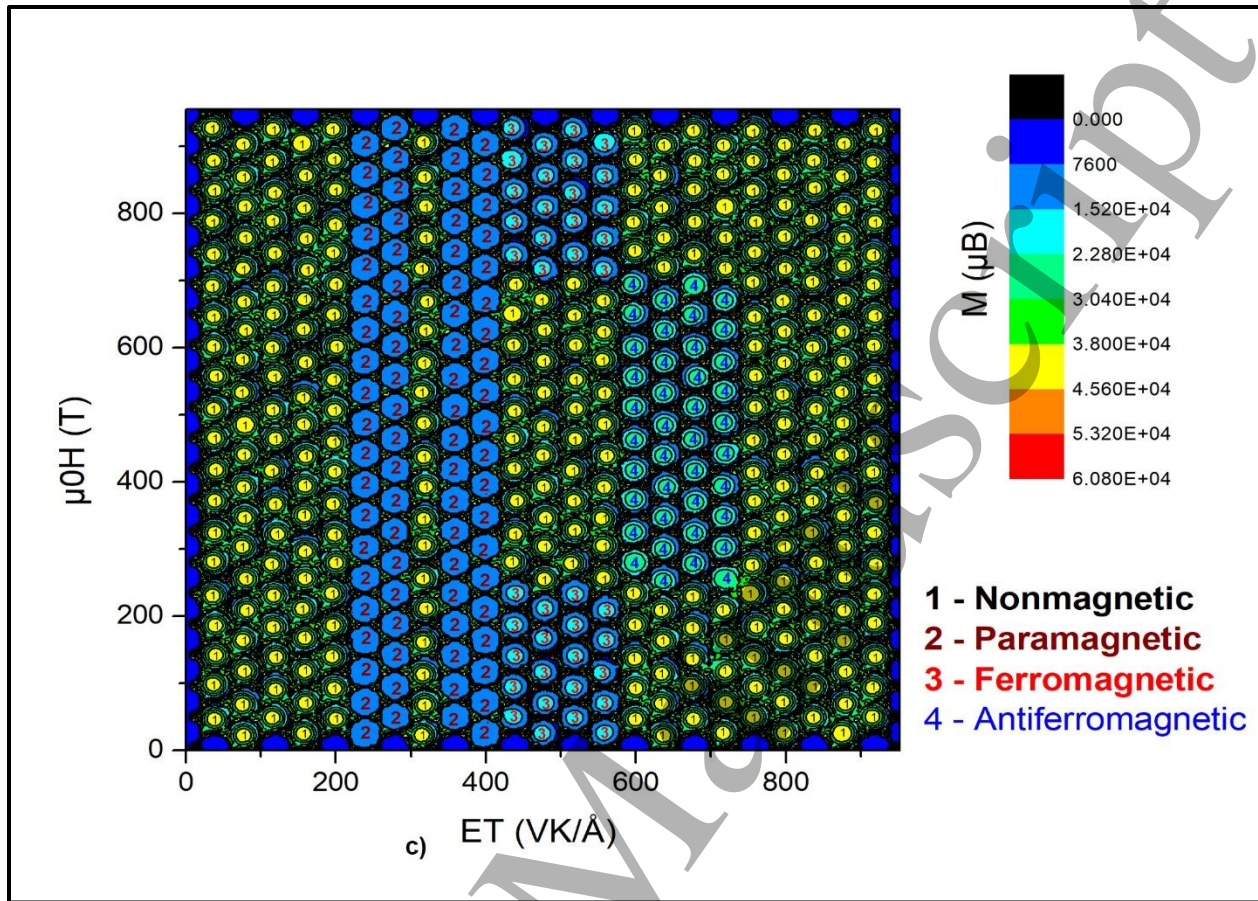


Figure 3. Magnetic phase diagram of a) 1x1nm b) 2.5x2.5 nm c) 5x5 nm szGNR. Contour plot of the product of electric field and temperature (ET product) vs. magnetic intensity vs. magnetization gives the magnetic phase transition from NM→PM→NM→PM→FM/NM/FM→NM/AFM/NM→NM in $n \times n$ nm szGNR where $n = \{1, 2.5, 5\}$. To distinguish the magnetic states it has been marked with numerals from 1,2,3,4 representing NM, PM, FM and AFM phases respectively.

3.4) Positional parameters study of the appeared magnetic phases: The contour plot of the magnetic phase diagram illustrated in Figure 3 clearly gives an overview of the magnetic phase existence and its positions. Positional parameters of the MPT have been extended for the conventional usage of szGNR ($n \times n$) of size 1nm to 50 nm. ET product values are obtained as illustrated in Figure 1 and mathematical expressions for calculating positional parameters and the magnetic phase existence have been briefly reported in the forthcoming Table 3.

Table 3. Total number of hexagons in X axis and Y axis[62] contributing towards each magnetic states and their existence range is represented here in their generic form for all $n \times n$ nm szGNRs where $n = \{1, 2, 3 \dots 50\}$. Mathematical expressions for number of hexagons and their positions for each corresponding state is shown; making this convention viable for real-time implementations.

No. of hexagons	Total number of hexagons		X axis (X_{Hex}) = $4.7n$; Y axis (Y_{Hex}) = $4n$; [For $n \times n$ dimension of pristine szGNR with their corresponding E, T; $n = \{1, 2, 3 \dots 50\}$]	
	X Axis	NM	$X_{NM} = 2n$;	
		PM,FM,AFM	For even n	$X_{PM, FM, AFM} = 0.9n$
			For odd n	$X_{PM} = 1n$ $X_{FM, AFM} = 0.85n$
	Y Axis	NM, PM	$Y_{NM, PM} = 4n$	
		FM,AFM	$Y_{FM} = 1n$ $Y_{AFM} = Y_{NM, PM} / 2$	
Position of hexagon (P)	X Axis	NM	[Position of X_{NM}] $P-X_{NM}\{s,m,e\}$; Start (s) and end ($e = P-X_{AFM} + X_{AFM}$) of the szGNR and in between positions (m) as mentioned below	
		PM	$P-X_{PM}\{a,b\}$ positions is $[\{(X_{NM}+1) \text{ to } (X_{NM} + (0.9n/3))\}, \{(X_{NM}+2(0.9n/3)+1) \text{ to } (X_{NM}+3(0.9n/3))\}]$; [The region (m) between these two positions is NM];	
		FM	$P-X_{FM} = P-X_{PM}\{b\} + 1$	
		AFM	$P-X_{AFM} = P-X_{FM} + X_{FM}$	
	Y Axis	NM	$P-Y_{NM} = P-X_{NM}\{s,m,e\}$	
		PM	$P-Y_{PM} = P-Y_{NM}\{s\} + 1$	
		FM	$P-Y_{FM}\{a,b\}$ position is $[\{(4n+1)-4n\} \text{ to } (Y_{FM})\}, \{(Y_{FM} + Y_{AFM} + 1) \text{ to } (4n)\}]$	

			[The region (m) between these two positions is NM];
		AFM	P- $Y_{AFM}\{a,b\}$ position is $\{(Y_{FM}+1) \text{ to } (Y_{FM} + Y_{AFM})\}$ [The region (m) below and above this position is NM].
Magnetic state ordering with respect to the direction of the applied field		$ \begin{array}{c} \mathbf{X\ axis} \\ \text{=====}>> \\ \mathbf{NM \rightarrow PM \rightarrow FM \rightarrow AFM \rightarrow NM} \\ << \text{=====} \\ \mathbf{ET} \qquad \qquad \qquad \mathbf{- X\ axis} \end{array} \tag{2} $	
Round off convention:			
a) If the final value is $< a.5$ round off to a and if it is $> a.5$ round off to a+1			
b) -1 to the value of X_{NM} and Y_{AFM} and -0.5 to the value of X_{Hex} when n is a decimal number			

Electron correlation calculations and the coupling constants have been calculated for $n \times n$ dimensions of szGNR to briefly report the positional parameters of the magnetic phase transitions happening in the graphene system with the applied ET. Figure 3. illustrates the Contour plot of the magnetic phase diagram occurring along their corresponding positions. Mathematical formulation have been reported for calculating the positional parameters tabulated in Table 3. To begin with, depending on the size of the szGNR the total number of hexagons needs to be calculated; upon calculation, total no of hexagons contributing towards each state NM, PM, FM, and AFM need to be analyzed. On knowing the existence of magnetic phases, its range is calculated within the total stipulated size of the szGNR. Mathematical expressions have been deduced for n as even, odd and decimal number enabling its multipurpose generic usage. Number of hexagons in x and y axis and their position calculations are repeated for both x and y axis.

Model numerical calculations for this mathematical expressions are given in Table S4 available as supplementary info. Figure S1 available in supplementary info shows how to analyze the number

1
2
3 of hexagons in szGNR as discussed in this letter. The molecular orbital spin, also accounts for this
4 unusual magnetic behavior exhibited. The zak and soliton phase paves the way for the symmetry
5 to be broken and causes degeneracy in the system inducing this magnetic nature in the single layer
6 zigzag graphene nanoribbons. Coupling effects of Electric field and Temperature: π electrons in
7 the carbon is non-trivially influenced by the zigzag edges. These constitute towards massless Dirac
8 fermion. 2 degrees of freedom is raised in association with 2 pseudo spins owing to szGNRs
9 bipartite lattice. The symmetry of the pseudospin Dirac fermion is broken apart due to the bipartite
10 lattice nature. Energy barrier between the magnetic phases is overcome by the assistance of
11 coupled effect of temperature and electric field. Local coordination of atoms (the length of the
12 bond) is measured by the distance between atomic nuclei. The coupling effect of electric field and
13 temperature breaks the symmetry by distorting the local coordination of atoms. Edge atoms plays
14 a major role in determining the intrinsic magnetic property of szGNR as the edge atoms majorly
15 contributes to the valence states which are nearer to the fermi level. The application of electric
16 field and temperature independently leads to FM and AFM magnetic phases. However the
17 coupling effects of electric field and temperature leads to the magnetic phase transitions with an
18 additional phase revelation. Re-Configurability of the system is also achieved as NM State appears
19 at the first and the end of the cycle. We envisage that the aforementioned points as the underlying
20 mechanism for this unusual MPT in szGNR.

21
22
23
24
25
26
27
28
29
30
31
32
33
34
35
36
37
38
39
40
41
42
43
44
45 3.5) Envisaged Application of the finding reported:
46
47
48
49
50
51
52
53
54
55
56
57
58
59
60

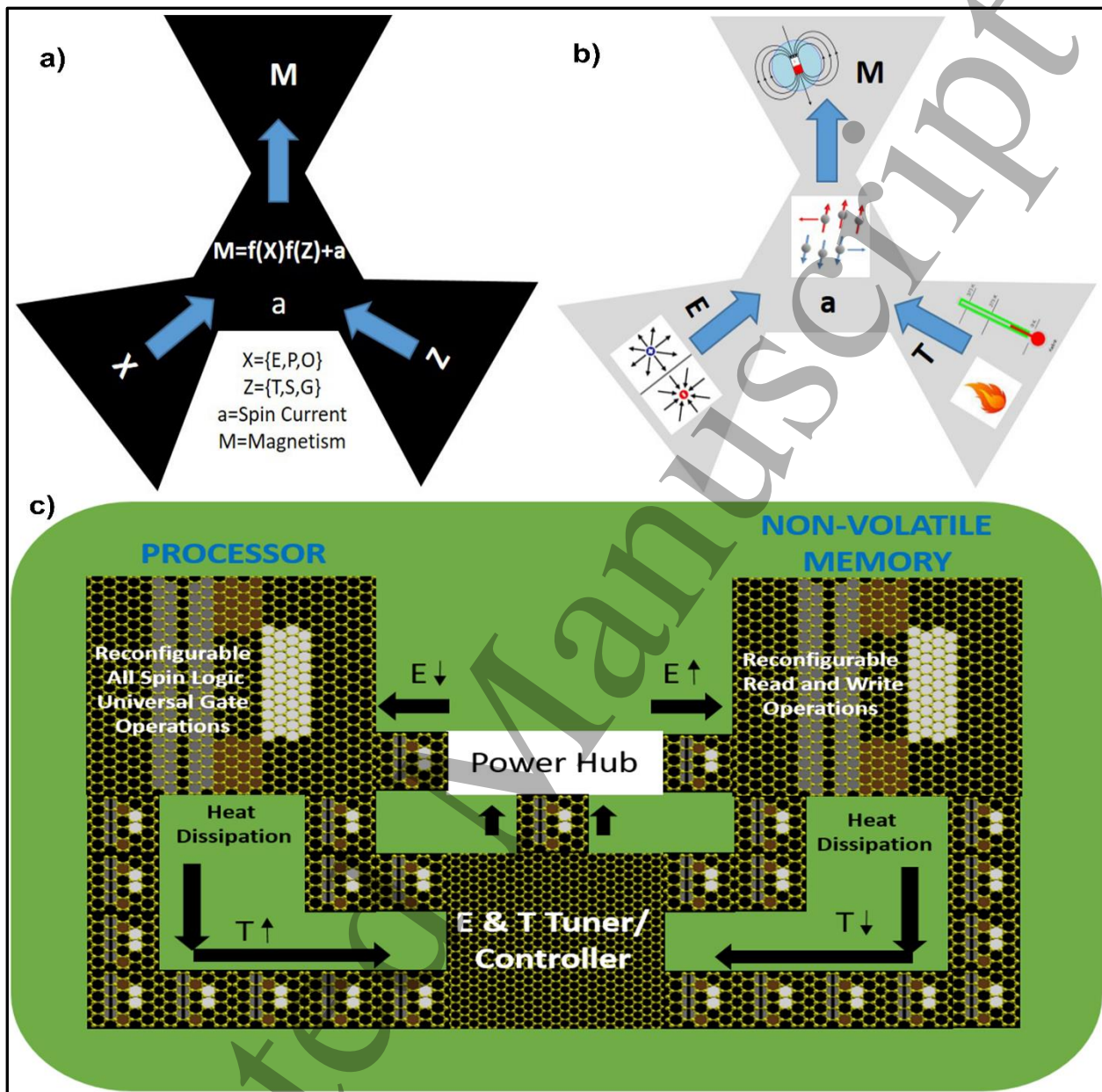


Figure 4. Proposed scheme and envisaged model a) proposed Bow-Tie schematic to induce intrinsic magnetism in carbon allotropes, where $X=\{E,P,O\}$ and $Z=\{T,S,G\}$ [M denotes magnetism, X , Z are set variables, a represents spin current, E is electric field, P is pressure, O is optical force, T is temperature, S is Strain and G is geometry]. b) Schematic for thermo electromagnetic effect described in this letter, where X and Z constitutes for E and T respectively c) Envisaged model of the processor application with szGNR of sizes 1×1 and 2.5×2.5 nm exhibiting tunable intrinsic magnetic phase transitions is reported here. E represents electric field in $V/\text{\AA}$ and T represents temperature in kelvin.

The proposed Bow-Tie scheme shown in Figure 4 (a,b) is expressed in Equation (3)

$$M = f(X)f(Z) + a \quad (3)$$

where $X=\{E,P,O\}$ and $Z=\{T,S,G\}$ [63][M denotes magnetism, X, Z are set variables, a represents spin current, E is electric field, P is pressure, O is optical force, T is temperature, S is Strain and G is geometry]. The proposed scheme for thermo electromagnetic effect; its general form for carbon allotropes and the envisaged device application in principle with the finding reported in this letter is presented in Figure 4. Bow Tie schematic is proposed to induce intrinsic magnetism in defect-free carbon allotropes, where the two tail ends count for the set variables. Dopants, vacancy, and defects commonly induce magnetism. This study aims to induce it by applying energy on pristine szGNR as defined in X and Z (the set variables). X and Z first influence the central part of the design. The change in the spin current constituting the central part of the Bow-Tie scheme plays a significant role in determining the induced magnetism. The head portion of the design portrays the induced magnetism by the combined influence of set variables X and Z in addition to the spin currents in the central region.

In specific to the finding here, the bow tie scheme is designed as in Figure 4(b) where the set variables X and Z are chosen as electric field in $V/\text{\AA}$ and temperature in kelvin, where \underline{a} is spin current by default. This scheme induces intrinsic magnetism in pristine szGNRs breaking the degeneracy of the system. With this proposed scheme, an envisaged model of the processor application has been presented as shown in Figure 4(c) Heat dissipation and low power consumption possess a major challenge in today's three dimensional (3D) electronics. To counter this, herein reported study on tunable magnetic phase transitions in pristine graphene by thermo electromagnetic effect is utilized. The two major operations involved in a Central Processing Unit (CPU) are data processing and data storage/retrieval[64]. Data processing generates much heat depending on the number of clock cycles and the logic. Therefore with the proposed design, when

1
2
3 the temperature is high; the electric field can be tuned to lower values, using an E and T controller.
4
5 The power will be regulated in the power hub and fed back to the processing block. Pristine
6
7 graphene can also be used for reconfigurable all spin logic universal gate operations which open
8
9 up new avenues for low power computing and graphene-based memory devices. In day to day
10
11 normal operations, the data storage/retrieval block that performs reconfigurable read and write
12
13 operations generates lesser heat compared to the processing block. When T is low, E should be
14
15 high and it is taken care of E and T controller and power is fed to the data storage/retrieval block
16
17 from the power hub. This feedback loop on both processing and memory block helps in catalyzing
18
19 this finding furthermore. In some instances, owing to extended read/write operations, it may also
20
21 emit lot of heat, then E will be automatically tuned to its lower value.
22
23
24
25

26
27 **4. CONCLUSION:** - Intrinsic magnetic phase transitions in szGNR, under the combined
28
29 influence of E and T (the thermo-electromagnetic effect), has been reported in this letter by using
30
31 DFT based first principle calculations. The spin orientations and the corresponding positional
32
33 parameters for this intrinsic magnetic phase transitions are also analyzed and reported for the first
34
35 time. The obtained results show that the novel scheme of applying E and T in combination
36
37 drastically tunes the magnetic properties of pristine szGNRs. The system changes from NM phase
38
39 to PM phase to FM phase to AFM phase and then finally to NM phase with the change in E and
40
41 T. The obtained results also conclude that E and T are inversely proportional to each other for
42
43 achieving intrinsic tunable magnetism reported here which can lead to novel electronic devices as
44
45 envisaged in this article. We also have built the theoretical model for noncollinear thermo-
46
47 electromagnetic effect, which predicts that the change in strain and or applied pressure equally
48
49 play an important role in further shaping the findings reported here. The effects of geometry and
50
51 defects along with tunable E and T are under study. The electric field at (2.4 V/Å) exhibits PM
52
53
54
55
56
57
58
59
60

1
2
3 phase, FM Phase and AFM Phase when $T=29, 124$ and 360 kelvin respectively. The minimum
4 amount of heat generated in a processor (T at 360 K) exhibits PM phase, FM phase, and AFM
5 phase when E is at $0.2, 0.6$ and 2.4 V/Å respectively. These results along with the controlled
6 tunableness pave the way towards the next generation low power computing paradigms.
7
8
9
10
11

12 ASSOCIATED CONTENT

13 Supporting Information:

14 The supporting information is available free of charge at DOI:

15
16
17
18
19 Details of the number of hexagons in X and Y-axis subjected to this calculation for various
20 pristine single layer zigzag graphene nanoribbons with their respective number of carbon atoms in
21 the unit cell used for simulation is discussed. Positional parameters calculations for 7.5×7.5 nm
22 and 10×10 nm is discussed and model mathematical calculation for positional parameters is solved.
23
24

25 AUTHOR INFORMATION

26 Corresponding Author

27 * Amit Acharyya, Department of Electrical Engineering, Indian Institute of Technology,
28 Hyderabad, India, E-mail: amit_acharyya@iith.ac.in.
29 ORCID: Amit Acharyya: 0000-0002-5636-0676
30
31

32 Author Contributions

33 S.S., S.D., carried out the density functional theory based first principle calculations. S.S. wrote
34 the paper. S.G.A. and A.A. supervised the study and revised the paper. All authors discussed the
35 results and commented on the manuscript. A.A. is the corresponding author.
36

37 Notes

38 The authors declare no competing financial interest.
39
40

41 ACKNOWLEDGMENT

42 Computational support on clusters at AESICD Laboratory IITH, HPC center IITH and the
43 National PARAM Supercomputing Facility (NPSF) PARAM Yuva II - Centre for Development
44 of Advanced Computing (CDAC) is gratefully acknowledged. The authors thank Anandkumar M,
45 Kannan PK, Karthikeyan R and Preethi S for their fruitful discussions. The authors acknowledge
46 the support from Visvesvaraya Young Faculty fellowship, MEITY, Govt of India and RedPine
47 Signals, USA.
48
49

50 REFERENCES:

- 51
52 [1] Novoselov K S, Geim A K, Morozov S V, Jiang D, Zhang Y, Dubonos S V, Grigorieva I V and Firsov A A 2004 Electric
53 field effect in atomically thin carbon films *Science* (80-.). **306** 666–9
54 [2] Wakabayashi K and Dutta S 2012 Nanoscale and edge effect on electronic properties of graphene *Solid State Commun.*
55 **152** 1420–30
56 [3] Castro Neto A H ., Peres N M R ., Novoselov K S ., Geim A K . and Guinea F 2009 The electronic properties of graphene
57 *Rev. Mod. Phys.* **81** 109–62
58
59
60

- 1
2
3 [4] Debroy S, Miriyala V P K, Sekhar K V, Acharyya S G and Acharyya A 2015 Graphene heals thy cracks *Comput. Mater. Sci.* **109** 84–9
- 4 [5] Nigar S, Zhou Z F, Wang H and Intiaz M 2017 Modulating the electronic and magnetic properties of graphene *Rsc Adv.* **7** 51546–80
- 5 [6] Fert A 2008 Nobel Lecture: Origin, development, and future of spintronics *Rev. Mod. Phys.* **80** 1517–30
- 6 [7] Pisani L, Chan J A, Montanari B and Harrison N M 2007 Electronic structure and magnetic properties of graphitic ribbons *Phys. Rev. B* **75**
- 7 [8] Barone V, Hod O and Scuseria G E 2006 Electronic structure and stability of semiconducting graphene nanoribbons *Nano Lett.* **6** 2748–54
- 8 [9] Santos H, Chico L and Brey L 2009 Carbon Nanoelectronics: Unzipping Tubes into Graphene Ribbons *Phys. Rev. Lett.* **103** 86801
- 9 [10] Capaz F J C and R B 2016 Effects of edge magnetism on the Kohn anomalies of zigzag graphene nanoribbons *Nanotechnology* **27** 65707
- 10 [11] Sepioni M, Nair R R, Rablen S, Narayanan J, Tuna F, Winpenny R, Geim A K and Grigorieva I V 2010 Limits on Intrinsic Magnetism in Graphene *Phys. Rev. Lett.* **105** 207205
- 11 [12] Gorjizadeh N, Ota N and Kawazoe Y 2013 Ground state analysis of magnetic nanographene molecules with modified edge *Chem. Phys.* **415** 64–8
- 12 [13] Sepioni M and GRIGORIEVA I I V 2013 *Magnetic properties of graphene* (UK: The University of Manchester, Manchester, UK)
- 13 [14] Sun L, Wei P, Wei J, Sanvito S and Hou S 2011 From zigzag to armchair: the energetic stability, electronic and magnetic properties of chiral graphene nanoribbons with hydrogen-terminated edges *J Phys Condens Matter* **23** 425301
- 14 [15] Zhou A, Sheng W and Xu S J 2013 Electric field driven magnetic phase transition in graphene nanoflakes *Appl. Phys. Lett.* **103**
- 15 [16] Brey L, Fertig H A and Das Sarma S 2007 Diluted graphene antiferromagnet *Phys Rev Lett* **99** 116802
- 16 [17] Nair R R, Sepioni M, Tsai I L, Lehtinen O, Keinonen J, Krasheninnikov A V, Thomson T, Geim A K and Grigorieva I V 2012 Spin-half paramagnetism in graphene induced by point defects *Nat. Phys.* **8** 199–202
- 17 [18] Ney A, Papakonstantinou P, Kumar A, Shang N-G and Peng N 2011 Irradiation enhanced paramagnetism on graphene nanoflakes *Appl. Phys. Lett.* **99**
- 18 [19] Rezapour M R, Yun J, Lee G and Kim K S 2016 Lower Electric Field-Driven Magnetic Phase Transition and Perfect Spin Filtering in Graphene Nanoribbons by Edge Functionalization *J Phys Chem Lett* **7** 5049–55
- 19 [20] Yun K-H, Lee M and Chung Y-C 2014 Electric field as a novel switch for magnetization of Fe/graphene system *J. Magn. Magn. Mater.* **362** 93–6
- 20 [21] Szałowski K 2015 Graphene nanoflakes in external electric and magnetic in-plane fields *J. Magn. Magn. Mater.* **382** 318–27
- 21 [22] Jing Li and Christophe Delerue Y-M N 2016 Manipulating Spin Polarization and Carrier Mobility in Zigzag Graphene Ribbons using an Electric Field *IEEE Int. Electron Devices Meet.* **3**
- 22 [23] Krompiewski S 2016 Edge magnetism of finite graphene-like nanoribbons in the presence of intrinsic spin-orbit interaction and perpendicular electric field *Nanotechnology* **27** 315201
- 23 [24] Şahin H, Senger R T and Ciraci S 2010 Spintronic properties of zigzag-edged triangular graphene flakes *J. Appl. Phys.* **108**
- 24 [25] Han W, Chen J R, Wang D, McCreary K M, Wen H, Swartz A G, Shi J and Kawakami R K 2012 Spin relaxation in single-layer graphene with tunable mobility *Nano Lett* **12** 3443–7
- 25 [26] Wang Z, Qin S and Wang C 2014 Electronic and magnetic properties of single-layer graphene doped by nitrogen atoms *Eur. Phys. J. B* **87**
- 26 [27] Dyrdał A and Barnaś J 2017 Anomalous, spin, and valley Hall effects in graphene deposited on ferromagnetic substrates *2D Mater.* **4** 34003
- 27 [28] Usachov D, Fedorov A, Otrokov M M, Chikina A, Vilkov O, Petukhov A, Rybkin A G, Koroteev Y M, Chulkov E V, Adamchuk V K, Gruneis A, Laubschat C and Vyalikh D V 2015 Observation of single-spin Dirac fermions at the graphene/ferromagnet interface *Nano Lett* **15** 2396–401
- 28 [29] Tridev Mishra et.al. 2017 Topological phase transitions in Graphene under periodic kicking *arxiv*
- 29 [30] Chen W, Yang Y, Zhang Z and Kaxiras E 2017 Properties of in-plane graphene/MoS₂ heterojunctions *2D Mater.* **4** 45001
- 30 [31] Hallal A, Ibrahim F, Yang H, Roche S and Chshiev M 2017 Tailoring magnetic insulator proximity effects in graphene: first-principles calculations *2D Mater.* **4** 25074
- 31 [32] Guo W S and Z Y N and Z Q Y and H 2010 Magnetism and perfect spin filtering effect in graphene nanoflakes *Nanotechnology* **21** 385201
- 32 [33] Lee H, Wakabayashi K, Son Y-W and Miyamoto Y 2012 A single particle Hamiltonian for electro-magnetic properties of graphene nanoribbons *Carbon N. Y.* **50** 3454–8
- 33 [34] Grujić M, Tadić M and Peeters F M 2013 Antiferromagnetism in hexagonal graphene structures: Rings versus dots *Phys. Rev. B* **87**
- 34 [35] Sheng K L and W 2015 Bias voltage control of magnetic phase transitions in graphene nanojunctions *Nanotechnology* **26** 345203
- 35
36
37
38
39
40
41
42
43
44
45
46
47
48
49
50
51
52
53
54
55
56
57
58
59
60

- [36] Vancsó P, Hagymási I and Tapasztó L 2017 A magnetic phase-transition graphene transistor with tunable spin polarization *2D Mater.* **4**
- [37] Alexandre S S, Lucio A D, Neto A H and Nunes R W 2012 Correlated magnetic states in extended one-dimensional defects in graphene *Nano Lett* **12** 5097–102
- [38] Lee H, Lee H-J and Kim S Y 2018 Room-temperature ferromagnetism from an array of asymmetric zigzag-edge nanoribbons in a graphene junction *Carbon N. Y.* **127** 57–63
- [39] Feldner H, Meng Z Y, Honecker A, Cabra D, Wessel S and Assaad F F 2010 Magnetism of finite graphene samples: Mean-field theory compared with exact diagonalization and quantum Monte Carlo simulations *Phys. Rev. B* **81**
- [40] Agapito L A and Kioussis N 2011 “Seamless” graphene interconnects for the prospect of all-carbon spin-polarized field-effect transistors *J Phys Chem C Nanomater Interfaces* **115** 2874–9
- [41] Di Paola C, D’Agosta R and Baletto F 2016 Geometrical Effects on the Magnetic Properties of Nanoparticles *Nano Lett* **16** 2885–9
- [42] Rao C N R, Matte H S S R, Subrahmanyam K S and Maitra U 2012 Unusual magnetic properties of graphene and related materials *Chem. Sci.* **3** 45–52
- [43] Chen L, Guo L, Li Z, Zhang H, Lin J, Huang J, Jin S and Chen X 2013 Towards intrinsic magnetism of graphene sheets with irregular zigzag edges *Sci Rep* **3** 2599
- [44] Kabir M and Saha-Dasgupta T 2014 Manipulation of edge magnetism in hexagonal graphene nanoflakes *Phys. Rev. B* **90**
- [45] Magda G Z, Jin X, Hagymasi I, Vancso P, Osvath Z, Nemes-Incze P, Hwang C, Biro L P and Tapasztó L 2014 Room-temperature magnetic order on zigzag edges of narrow graphene nanoribbons *Nature* **514** 608–11
- [46] Delplace P, Ullmo D and Montambaux G 2011 Zak phase and the existence of edge states in graphene *Phys. Rev. B* **84**
- [47] Chen W C, Zhou Y, Yu S L, Yin W G and Gong C D 2017 Width-Tuned Magnetic Order Oscillation on Zigzag Edges of Honeycomb Nanoribbons *Nano Lett* **17** 4400–4
- [48] López-Sancho M P and Brey L 2017 Charged topological solitons in zigzag graphene nanoribbons *2D Mater.* **5**
- [49] Zhang T, Wu S, Yang R and Zhang G 2017 Graphene: Nanostructure engineering and applications *Front. Phys.* **12**
- [50] Huang W M, Hikihara T, Lee Y C and Lin H H 2017 Edge magnetism of Heisenberg model on honeycomb lattice *Sci Rep* **7** 43678
- [51] Debroy S, Kumar V P, Sekhar K V, Acharyya S G and Acharyya A 2017 Synergistic effect of temperature and point defect on the mechanical properties of single layer and bi-layer graphene *Superlattices Microstruct.* **110** 205–14
- [52] Berger D S and S O V and D M and C H M and E E F and P F and J M and P V and S M and P P and B H and A D K and T J and O G and C G K and A 2017 The 2017 Magnetism Roadmap *J. Phys. D: Appl. Phys.* **50** 363001
- [53] M T Carroll R F W B and S H V 1986 Local and non-local spin density functional calculations of the correlation energy of atoms in molecules *J. Phys. B At. Mol. Phys.* **20** 3599–629
- [54] Giannozzi P, Baroni S, Bonini N, Calandra M, Car R, Cavazzoni C, Ceresoli D, Chiarotti G L, Cococcioni M, Dabo I, Dal Corso A, de Gironcoli S, Fabris S, Fratesi G, Gebauer R, Gerstmann U, Gougoussis C, Kokalj A, Lazzeri M, Martin-Samos L, Marzari N, Mauri F, Mazzarello R, Paolini S, Pasquarello A, Paulatto L, Sbraccia C, Scandolo S, Sclauzero G, Seitsonen A P, Smogunov A, Umari P and Wentzcovitch R M 2009 QUANTUM ESPRESSO: a modular and open-source software project for quantum simulations of materials *J Phys Condens Matter* **21** 395502
- [55] Giannozzi P, Andreussi O, Brummé T, Bunau O, Buongiorno Nardelli M, Calandra M, Car R, Cavazzoni C, Ceresoli D, Cococcioni M, Colonna N, Carnimeo I, Dal Corso A, de Gironcoli S, Delugas P, DiStasio R A, Ferretti A, Floris A, Fratesi G, Fugallo G, Gebauer R, Gerstmann U, Giustino F, Gorni T, Jia J, Kawamura M, Ko H Y, Kokalj A, Küçükbenli E, Lazzeri M, Marsili M, Marzari N, Mauri F, Nguyen N L, Nguyen H V, Otero-de-la-Roza A, Paulatto L, Poncé S, Rocca D, Sabatini R, Santra B, Schlipf M, Seitsonen A P, Smogunov A, Timrov I, Thonhauser T, Umari P, Vast N, Wu X and Baroni S 2017 Advanced capabilities for materials modelling with Quantum ESPRESSO *J. Phys. Condens. Matter* **29**
- [56] John P. Perdew Matthias Ernzerhof K B 1996 Generalized Gradient Approximation Made Simple *Phys. Rev. Lett.* **77**
- [57] Laasonen K, Pasquarello A, Car R, Lee C and Vanderbilt D 1993 Car-Parrinello molecular dynamics with Vanderbilt ultrasoft pseudopotentials *Phys. Rev. B* **47** 10142–53
- [58] Alessandro Curioni and Max Planck Institute S 2000 CPMD
- [59] Reddy R P, Acharyya A and Khurshed S 2017 A Cost-Effective Fault Tolerance Technique for Functional TSV in 3-D ICs *IEEE Trans. Very Large Scale Integr. Syst.* **25** 2071–80
- [60] Györffy J S and B L 1999 A note on a wavefunction formulation of the Korringa–Kohn–Rostoker method for calculating the electronic structure of layered systems *J. Phys. Condens. Matter* **11** 7125–7142
- [61] Chen C-W 1977 CHAPTER 4 - MAGNETIC PROPERTIES *Magnetism and Metallurgy of Soft Magnetic Materials* (Elsevier) pp 98–170
- [62] Kokalj A 2003 Computer graphics and graphical user interfaces as tools in simulations of matter at the atomic scale *Comput. Mater. Sci.* **28** 155–68
- [63] Kou L, Tang C, Zhang Y, Heine T, Chen C and Frauenheim T 2012 Tuning Magnetism and Electronic Phase Transitions by Strain and Electric Field in Zigzag MoS₂ Nanoribbons *J. Phys. Chem. Lett.* **3** 2934–41
- [64] Hennessy J L and Patterson D A 2011 *Computer Architecture, Fifth Edition: A Quantitative Approach* (Morgan Kaufmann Publishers Inc.)